THE EFFECT OF SOLUTION TREATMENT TEMPERATURE ON PROPERTIES OF Ti-Nb-Zr ALLOY FOR BIOAPPLICATIONS

MÁLEK Jaroslav[1], HNILICA František[1], VESELÝ Jaroslav[1], VLACH Martin[2], KOLAŘÍK Kamil[3]

[1]*UJP PRAHA a.s., Prague, Czech Republic, EU, malek@ujp.cz*
[2]*Charles University, Faculty of Mathematics and Physics, Prague, Czech Republic, EU, martin.vlach@mff.cuni.cz*
[3]*CTU in Prague, Prague, Czech Republic, EU*

Abstract

The beta-titanium alloys are used for bioapplications (e.g. orthopaedic or dental implants) due to their excellent properties like biocompatibility, corrosion resistance, high strength, low Young's modulus). The processing of these alloys is essential for their properties and therefore processing parameters should be chosen properly. In this work the effect of solution treatment temperature on properties of Ti-35Nb-Zr alloys has been studied by means of light microscopy, X-ray diffraction analysis and DSC analysis. The Ti-35Nb-2Zr alloy was prepared through powder metallurgy process (blended elemental powders, cold isostatic pressing and sintering). Sintered specimens were hot forged and solution treated at temperatures 800, 850, 900, 950 and 1000 °C for 0.5 hrs and water quenched. The grain size changed from 35 to 75 μm. In addition precipitation processes have been observed along with precipitate coarsening. The α-phase precipitation has significant influence on the matrix grain growth.

Keywords: Solution treatment, beta-titanium, grain size, powder metallurgy

1. INTRODUCTION

Titanium alloys are used as construction materials in automotive and aerospace industry for many years thanks to their superior properties (i.e. high strength, low density or good corrosion resistance). These properties also predict them for use in biomedical applications [1, 2]. The pure titanium (grade 2) is used for implants not bearing significant load due to its lower tensile strength. The most common Ti6Al4V alloy is used for implants instead of AISI 316L stainless steel. The Ti6Al4V alloy has significantly lower elastic modulus (110 GPa) than stainless steels or Co-Cr alloys (> 200 GPa), but the Young's modulus is still far higher than that of bone (10-40 GPa) [1, 3]. Higher Young's modulus of implant than that of bone may cause the so called "stress-shielding effect" [4]. The load is transmitted mainly by the implant and only small part by the bone. The bone is not sufficiently loaded which may cause atrophy and bone loosening. The currently used AISI 316L stainless steel or Ti6Al4V alloy contain elements with problematic biocompatibility (i.e. Cr, Al and V) and therefore the development of new materials with lower Young's modulus and superior biocompatibility took place. The most promising candidates are beta-titanium alloys with fully biocompatible elements (e.g. Nb, Ta, Zr) [4, 5]. The beta-titanium alloys may have low modulus (as low as 50 GPa) and high strength. Processing parameters can significantly influence the resulting mechanical properties of the alloy and therefore their control is essential for technological processes. One of the most important technological parameter is a solution treatment temperature. This parameter is connected with α/β transition temperature and depends on chemical composition. Particularly interstitial elements (e.g. O, N) strongly influence this parameter [6 - 8]. The aim of this work was to describe the influence of various solution temperatures on properties of Ti-35Nb-2Zr alloy prepared by powder metallurgy process.

2. EXPERIMENTAL

The beta-titanium alloy with nominal chemical composition Ti-35Nb-2Zr (all compositions in this paper are in wt.%) was prepared via powder metallurgy process. Elemental powders were used with purity of at least 99.5% and grain size -325 mesh (i.e. < 44 μm) were mixed filled in moulds. Those operations have been performed under protective Ar atmosphere. Specimens were cold isostatically pressed (CIP) at 400 MPa and subsequently sintered. Sintering has been carried out in a vacuum furnace. At first specimens were heated up to 800 °C and hold for 1 hour and subsequently heated to sintering temperature 1300 °C and sintered for 20 hours. Sintered specimens were machined into cylinders of about 33 mm in diameter and swaged at 1000 °C to 12 mm diameter (in multiple steps). Swaged specimens were annealed at various temperatures (800, 850, 900, 950 and 1000 °C) for 0.5 h and water quenched. The oxygen content in final alloy has been determined by Bruker Galileo G8 gas fusion analyzer to 0.48 wt.%.

The microstructure has been studied by light microscopy, Scanning electron microscopy (JEOL JSM 7600F with Oxford X-max EDS detector). Also the electron back scatter diffraction (EBSD) detector was used for further analysis. EBSD data were processed in HKL Channel 5 software package. The samples for light microscopy were prepared via a standard metallographic process (grinded up to #4000 with SiC papers and polished with Struers OP-S emulsion with the addition of H_2O_2). 3 ml HF + 8 ml HNO_3 + 100 ml H_2O etchant was used for etching. X-ray diffraction (XRD) measurements were performed on an X'Pert PRO diffractometer equipped with a 1D detector and Cu K-α radiation. The TOPAS program was used for Rietveld refinement of the diffraction pattern.

3. RESULTS AND DISCUSSION

The typical microstructure of as sintered specimen is shown in **Figure 1**. Certain amount of residual porosity (about 3 vol.%) can be seen in **Figure 1** along with equiaxed β-grains. The grey areas are supposed to be α-precipitates as was observed also in previous papers in similar alloys [9]. Pores were completely removed during hot deformation (see **Figure 2**) and also the grain size has been significantly reduced from 120 μm to 40 μm due to dynamic recrystallization processes. The different shades of gray colour in micrograph (**Figure 2a**) are caused by different etching that may arise due to the presence of deformation effects (high dislocation density, substructure). The fact that substructure is present in hot swaged (hot deformed) specimens was also revealed by the EBSD analysis (**Figure 2b**). Moreover certain amount of fine precipitates may also contribute to different etching, but those precipitates were not observed by used techniques. The LM resolution is not good enough to reveal the fine precipitates nor was the XRD analysis (revealed only the β-phase).

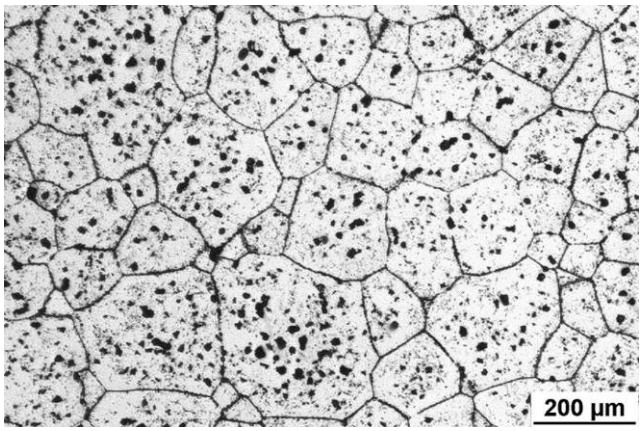

Figure 1 The microstructure of as-sintered specimen

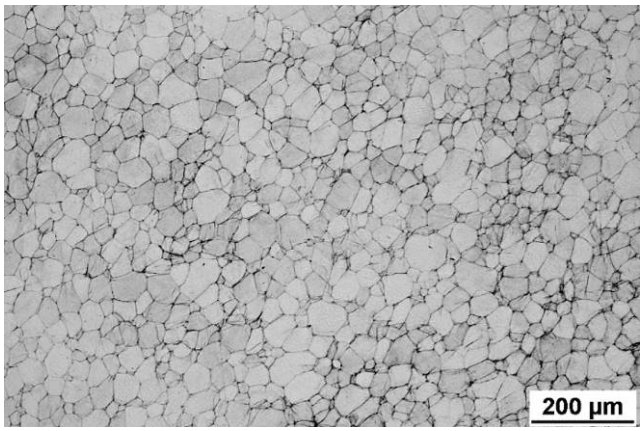

Figure 2a The microstructure of hot forged specimen

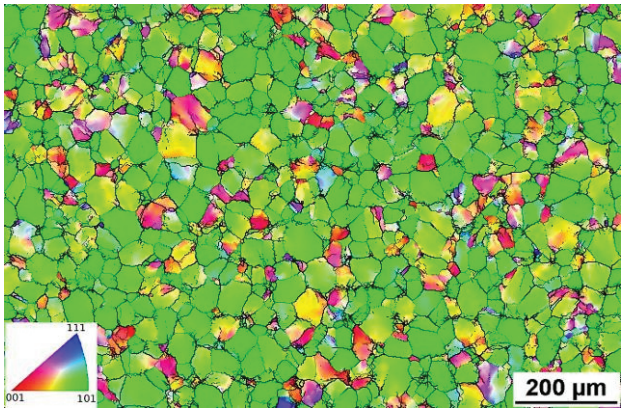

Figure 2b Inverse pole figure (IPF) map of hot swaged specimen (swaging axis perpendicular to screen)

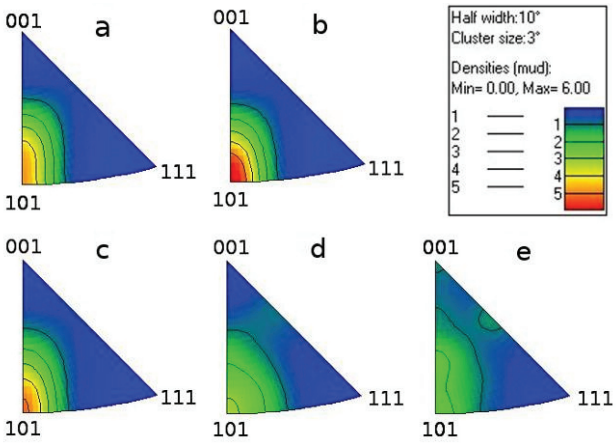

Figure 3 IPF (swaging axis) of a) hot swaged; b) 800 °C annealed; c) 850 °C annealed; d) 900 °C annealed and e) 950 °C annealed specimens

More profound studies are planned to be performed in future. On the other hand the presence of fine precipitates cannot be expelled due to slower cooling rate from swaging temperature. The EBSD analysis also revealed that the {110} (plane perpendicular to swaging axis) texture also emerged during the hot deformation process (see **Figure 3** - inset a).The effect of solution treatment temperature can be observed in **Figure 4** where microstructures of annealed (at different temperatures) and water quenched specimens are presented. The microstructure of 800 °C annealed specimen consists of equiaxed grains with fine precipitates throughout the specimen (both inside grains and along grain boundaries). Locally areas with lower number of precipitates can be seen. It has been determined by EDS analysis that those places contain slightly higher amount of Nb. The increase in Nb amount is approximately 1 wt.% measured by EDS analysis. Niobium is known to act as a β-stabilizer in Ti alloys and therefore it can be assumed that this slight increase in Nb content hindered the α-precipitation during annealing. The areas with slightly increased Nb content are probably the original positions of Nb grains in specimen after cold isostatic pressing. It seems that slight concentration differences remained in the specimen after sintering and swaging. Even such a small difference may cause different precipitation. The relatively strong {110} texture was still observed after 800 °C annealing. In 850 °C annealed specimen the precipitates are mainly distributed on grain boundaries and their volume fraction is significantly lower than in 800 °C annealed specimen. Precipitate free zones (with respect to LM resolution) can be also observed (similarly to 800 °C specimen). In these areas the grains are significantly coarser and non-deformed (as is evident from **Figure 4b**). The grain growth is allowed by precipitate coarsening (and precipitate dissolution) as the precipitates become unable to pin up the grain boundaries. This can be confirmed by **Figure 4f**, where precipitates along original grain boundary can be observed. It can be therefore assumed that the grain coarsening does not occur in places where precipitates are present. The {110} texture can still be observed (**Figure 3**), because the majority of the specimen contains precipitates (along grain boundaries) and therefore the volume fraction of fully recrystallized grains is low. Further temperature increase lead to complete precipitate dissolution in 900 °C annealed specimen. Coarse recrystallized grains can be observed in **Figure 4c**. No substructure or deformation has been observed in those grains and also the {110} texture became much weaker than in specimens annealed at lower temperatures. However even at higher annealing temperature (950 °C) weak {110} recrystallization texture is present (see **Figure 3**). The grain size vs. annealing temperature dependence is plotted in **Figure 5**. It is evident that the average grain size of hot forged, 800 °C and 850 °C annealed specimens is about 40 µm. Sharp increase in grain size can be observed at temperatures above 850 °C, when the grain size of 900 °C is about 55 µm and at higher temperature the grain size reaches 80 µm. This is consistent with the precipitate dissolution and subsequent grain growth.

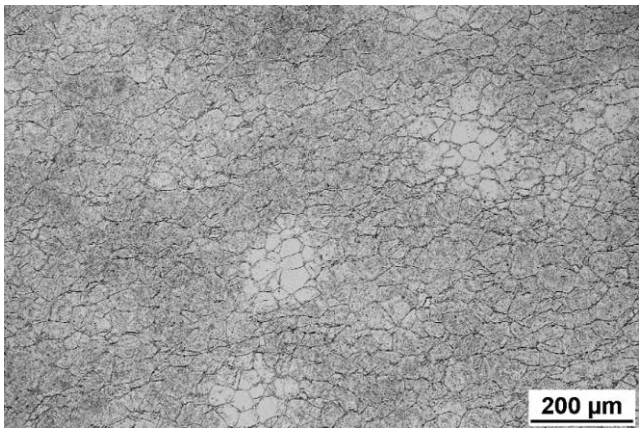

Figure 4a The microstructure of 800 °C annealed specimen

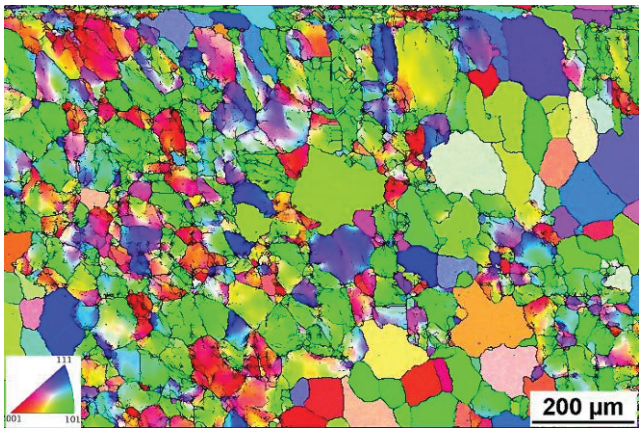

Figure 4b The microstructure of 850 °C annealed specimen (EBSD-IPF)

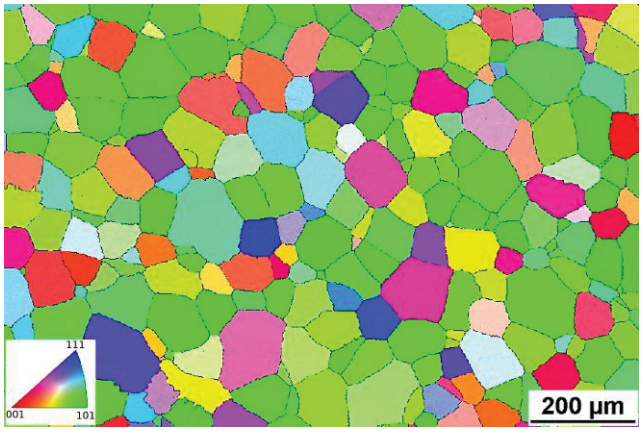

Figure 4c The microstructure of 900 °C annealed specimen (EBSD-IPF)

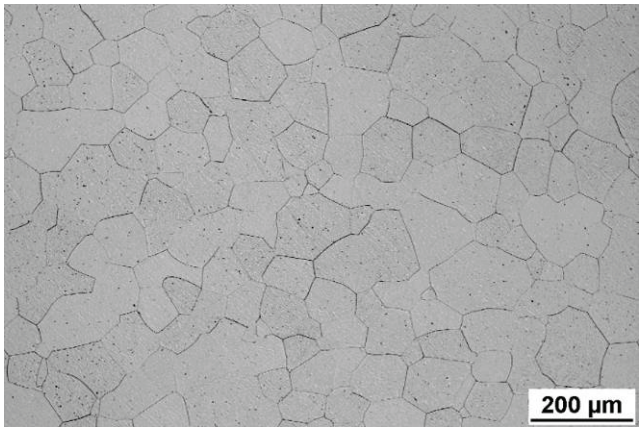

Figure 4d The microstructure of 950 °C annealed specimen

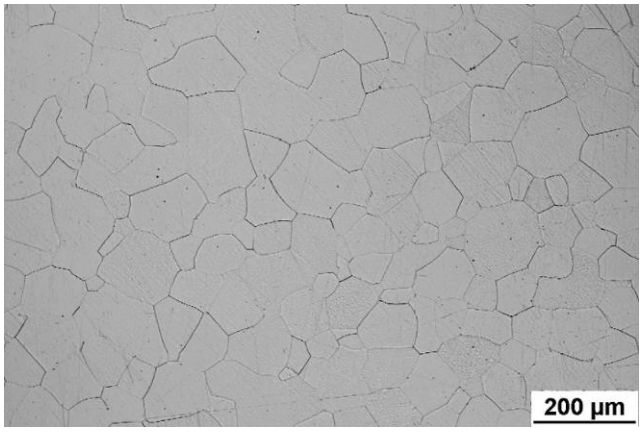

Figure 4e The microstructure of 1000 °C annealed specimen

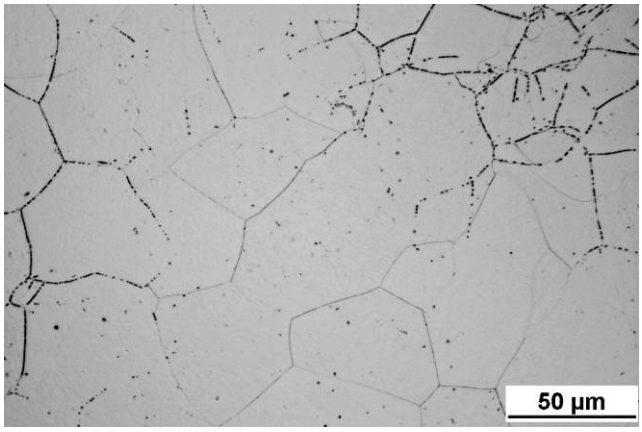

Figure 4f The microstructure of 850 °C annealed specimen-detail

The precipitate dissolution takes place above the α/β transition temperature. Along to our observations it can be assumed that the α/β transition temperature is between 850 °C and 900 °C for the studied alloy as no precipitates were observed in 900 °C annealed specimen. On the other hand some precipitates along grain

boundaries can be observed in 850 °C annealed specimen. It should be pointed out that the real α/β transition temperature is probably even slightly lower, because in this case only 0.5 h annealing period was used, which possibly does not need to be sufficient for complete precipitate dissolution. Some authors reported theoretical models on determining the α/β transition temperature [8, 10 - 12]. Okazaki et al. [10] reported a model along which the α/β transition temperature for the current alloy should be 802 °C which is close to Geng et al. [8] (785 °C) and these values seem to be close to our observations. On the other hand some authors reported models that give lower values (e.g. 680 °C [11]).

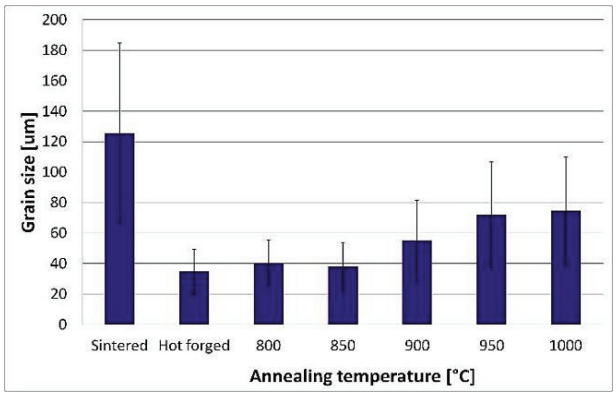

Figure 5 The grain size of studied specimens

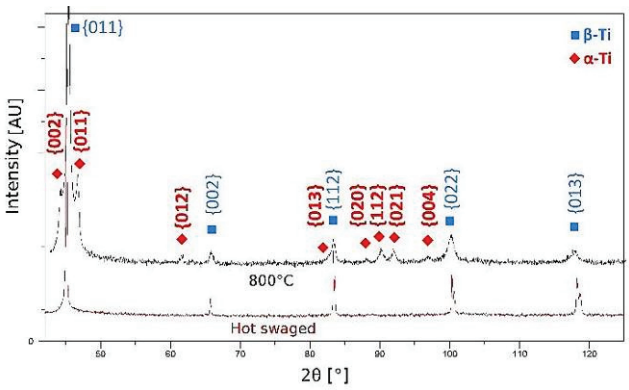

Figure 6 The XRD profiles of hot swaged and 800 °C annealed specimens

The presence of α-precipitates in 800 °C annealed specimen was confirmed also by XRD analysis (**Figure 6**). The α-phase precipitated during heating and (for temperatures lower than α/β transition temperature) at annealing temperature. It has been reported that in similar alloys precipitation starts at temperatures about 300 °C (ω-precipitation) and continues up to α/β transition temperature. Moreover significant precipitate coarsening may occur at higher temperatures [7, 13 - 15]. More detailed study is planned in future to elucidate the precipitation processes by using more precise methods (e.g. transmission electron microscopy). The precipitation probably starts at grain boundaries as they are areas with higher energy.

4. CONCLUSIONS

The effect of solution treatment temperature has been studied. On the basis of obtained results can be concluded that:

1) Residual porosity was removed and significant grain refinement was achieved during hot forging process.
2) Static recrystallization occurred during solution treatment. Grain coarsening has been hindered by α-precipitates.
3) During annealing above α/β transition temperature significant grain coarsening took place.
4) {110} texture emerged during hot swaging.

ACKNOWLEDGEMENTS

Authors would like to express gratitude for financial support of this work to Technology Agency of the Czech Republic project No. TE01020390.

REFERENCES

[1] ZHAO, X., NIINOMI, M., NAKAI, M., MIYAMOTO, G., FURUHARA, T. Microstructures and mechanical properties of metastable Ti-30Zr-(Cr, Mo) alloys with changeable Young's modulus for spinal fixation applications. *Acta Biomater.*, 2011, vol. 7, no. 8, pp. 3230-3236.

[2] LONG, M., RACK, H. J. Titanium alloys in total joint replacement--a materials science perspective. *Biomaterials*, 1998, vol. 19, no. 18, pp. 1621-1639.

[3] BÖNISCH, M. CALIN, M., VAN HUMBEECK, J., SKROTZKI, W., ECKERT, J. Factors influencing the elastic moduli, reversible strains and hysteresis loops in martensitic Ti-Nb alloys. *Mater. Sci. Eng. C*, 2015, vol. 48, pp. 511-520.

[4] WILLIAMS, D. F. On the mechanisms of biocompatibility. *Biomaterials*, 2008, vol. 29, no. 20, pp. 2941-2953.

[5] BIESIEKIERSKI, A., WANG, J., ABDEL-HADY GEPREEL, M., WEN, C. A new look at biomedical Ti-based shape memory alloys. *Acta Biomater.*, 2012, vol. 8, no. 5, pp. 1661-1669.

[6] MÁLEK, J., HNILICA, F., VESELÝ, J., ŘÍHOVÁ, Z. The effect of intersticial elements O and B on transition temperature (α - β) of Ti-35Nb-6Ta biomedical alloy. In *METAL 2014,* Conference Proceedings, Ostrava: TANGER, 2014, pp. 1116-1121.

[7] AROCKIAKUMAR, R., PARK, J. K. Effect of α-precipitation on the superelastic behavior of Ti-40wt.%Nb-0.3wt.%O alloy processed by equal channel angular extrusion. *Mater. Sci. Eng. A*, 2010, vol. 527, no. 10-11, pp. 2709-2713.

[8] GENG, F., NIINOMI, M., NAKAI, M. Observation of yielding and strain hardening in a titanium alloy having high oxygen content. *Mater. Sci. Eng. A*, 2011, vol. 528, no. 16-17, pp. 5435-5445.

[9] MÁLEK, J., HNILICA, F., VESELÝ, J. Influence of grain size on microstructure and porosity of biocomptible Ti-35.5Nb-5.,7Ta alloy processed via powder metallurgy. In *METAL 2010: 19th International Conference on Metallurgy and Materials,* Conference Proceedings, Ostrava: TANGER, 2010, pp. 855-860.

[10] OKAZAKI, Y., ITO, Y., ITO, A., TATEISHI, T. Effect of alloying elements on mechanical properties of titanium alloys for medical implants. *Materials Transactions, JIM*, 1993, vol. 34, no. 12. pp. 1217-1222.

[11] LI, S., HAO, Y., YANG, R., CUI, Y., NIINOMI, M. Effect of Nb on microstructural characteristics of Ti-Nb-Ta-Zr alloy for biomedical applications. *Mater. Trans.*, 2002, vol. 43, no. 12, pp. 2964-2969.

[12] GUO, W. Y., XING, H., SUN, J., LI, X. L., WU, J. S., CHEN, R. Evolution of microstructure and texture during recrystallization of the cold-swaged Ti-Nb-Ta-Zr-O alloy. *Metall. Mater. Trans. A Phys. Metall. Mater. Sci.*, 2008, vol. 39 A, no. 3, pp. 672-678.

[13] CREMASCO, A., ANDRADE, P. N., CONTIERI, R. J., LOPES, E. S. N., AFONSO, C. R. M., CARAM, R. Correlations between aging heat treatment, ?? phase precipitation and mechanical properties of a cast Ti-Nb alloy. *Mater. Des.*, 2011, vol. 32, no. 4, pp. 2387-2390.

[14] AFONSO, C. R. M., FERRANDINI, P. L., RAMIREZ, A. J., CARAM, R. High resolution transmission electron microscopy study of the hardening mechanism through phase separation in a ??-Ti-35Nb-7Zr-5Ta alloy for implant applications. *Acta Biomater.*, 2010, vol. 6, no. 4, pp. 1625-1629.

[15] MANTANI, Y., TAJIMA, M. Phase transformation of quenched α'' martensite by aging in Ti-Nb alloys. *Mater. Sci. Eng. A*, 2006, vol. 438-440, pp. 315-319.